Supplementary Materials for

"Penetration and intrusion of weak symmetric plane fountains in linearly stratified fluids"

M. I. Inam[a], Wenxian Lin[b,†], S. W. Armfield[c], and Mehdi Khatamifar[b]

[a] Department of Mechanical Engineering, Khulna University of Engineering and Technology, Khulna, 9203, Bangladesh

[b] College of Science, Technology & Engineering, James Cook University, Townsville, QLD 4811, Australia

[c] School of Aerospace, Mechanical and Mechatronic Engineering, The University of Sydney, NSW 2006, Australia

[†] Corresponding author: Email: wenxian.lin@jcu.edu.au (W. Lin)

March 8, 2023

1 Methodology

The physical system under consideration is a rectangular container of the dimensions $H \times B \times L$ (Height $\times$ Width $\times$ Length), containing a Newtonian fluid initially at rest and with a constant temperature gradient $dT_{a,z}/dZ$, as sketched in Fig. 1. At the center of the bottom of the container, a narrow slot with a half-width of X_0 in the Y direction functions as the source for a plane fountain, with the remainder of the bottom being a rigid, non-slip and adiabatic surface. The two vertical surfaces in the $X - Z$ plane, at $Y = \pm B/2$, are assumed to be periodic whereas the two vertical surfaces in the $Y - Z$ plane, at $X = \pm L/2$, are assumed to be outflows. The top surface in the $X - Y$ plane, at $Y = H$, is assumed to be a wall. The origin of the Cartesian coordinate systems is at the center of the bottom. The gravity is acting in the negative Z-direction. At time $t = 0$, a stream of fluid at T_0 ($T_0 < T_{a,0}$) is injected upward from the slot with a uniform velocity W_0 into the container to initiate the plane fountain flow and this discharge is maintained over the whole course of a specific numerical simulation run.

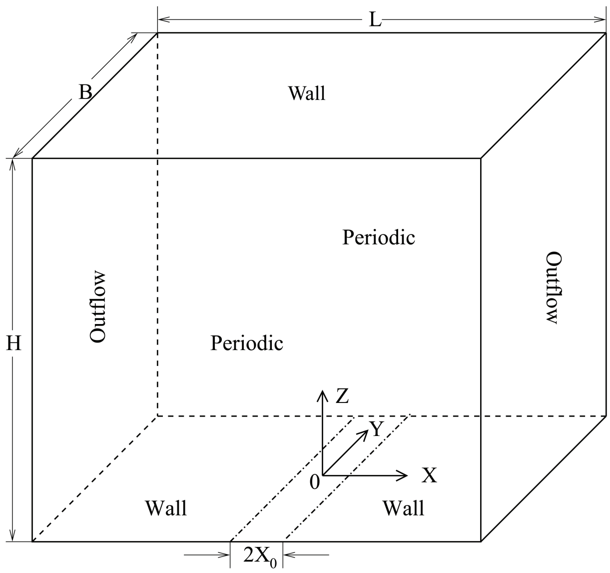

Figure S1: Sketch of the physical system under consideration, the computational domain and the boundary conditions.

The flow is governed by the three-dimensional incompressible Navier-Stokes and temperature equations with the Oberbeck-Boussinesq approximation, which are written in conservative form in Cartesian coordinates as follows,

$$\frac{\partial U}{\partial X} + \frac{\partial V}{\partial Y} + \frac{\partial W}{\partial Z} = 0, \tag{1}$$

$$\frac{\partial U}{\partial t} + \frac{\partial (UU)}{\partial X} + \frac{\partial (VU)}{\partial Y} + \frac{\partial (WU)}{\partial Z} = -\frac{1}{\rho}\frac{\partial P}{\partial X} + \nu\left(\frac{\partial^2 U}{\partial X^2} + \frac{\partial^2 U}{\partial Y^2} + \frac{\partial^2 U}{\partial Z^2}\right), \tag{2}$$

$$\frac{\partial V}{\partial t} + \frac{\partial (UV)}{\partial X} + \frac{\partial (VV)}{\partial Y} + \frac{\partial (WV)}{\partial Z} = -\frac{1}{\rho}\frac{\partial P}{\partial Y} + \nu\left(\frac{\partial^2 V}{\partial X^2} + \frac{\partial^2 V}{\partial Y^2} + \frac{\partial^2 V}{\partial Z^2}\right), \tag{3}$$

$$\begin{aligned}\frac{\partial W}{\partial t} + \frac{\partial (UW)}{\partial X} + \frac{\partial (VW)}{\partial Y} + \frac{\partial (WW)}{\partial Z} &= -\frac{1}{\rho}\frac{\partial P}{\partial Z} + \nu\left(\frac{\partial^2 W}{\partial X^2} + \frac{\partial^2 W}{\partial Y^2} + \frac{\partial^2 W}{\partial Z^2}\right)\\ &\quad + g\beta(T - T_{a,Z}),\end{aligned} \tag{4}$$

$$\frac{\partial T}{\partial t} + \frac{\partial (UT)}{\partial X} + \frac{\partial (VT)}{\partial Y} + \frac{\partial (WT)}{\partial Z} = \kappa\left(\frac{\partial^2 T}{\partial X^2} + \frac{\partial^2 T}{\partial Y^2} + \frac{\partial^2 T}{\partial Z^2}\right), \tag{5}$$

where U, V, and W are the velocity components in the X, Y, and Z directions, t is time, P is pressure, T is temperature, and ρ, ν, and κ are the density, viscosity, and thermal diffusivity of fluid, respectively.

The appropriate initial and boundary conditions are:

$$U = V = W = 0,\ \ T(Z) = T_{a,0} + s(T_{a,0} - T_0)\frac{Z}{X_0} \ \text{ at all } \ X, Y, Z,$$

when $t < 0$, and

$$\begin{gathered}
U = V = 0,\ \ W = W_0,\ \ T = T_0 \ \text{ at } \ Z = 0,\ \ -X_0 \le X \le X_0 \ \text{ and } \ -\frac{B}{2} \le Y \le \frac{B}{2};\\
U = V = W = 0,\ \ \frac{\partial T}{\partial Z} = 0 \ \text{ at } \ Z = 0,\ \ X_0 \le X \le \frac{L}{2} \ \text{ and } \ -\frac{B}{2} \le Y \le \frac{B}{2};\\
U = V = W = 0,\ \ \frac{\partial T}{\partial Z} = 0 \ \text{ at } \ Z = 0,\ \ -\frac{L}{2} \le X \le -X_0 \ \text{ and } \ -\frac{B}{2} \le Y \le \frac{B}{2};\\
U = V = W = 0,\ \ \frac{\partial T}{\partial Z} = 0 \ \text{ at } \ Z = H,\ \ -\frac{L}{2} \le X \le \frac{L}{2} \ \text{ and } \ -\frac{B}{2} \le Y \le \frac{B}{2};\\
\frac{\partial U}{\partial X} = \frac{\partial V}{\partial X} = \frac{\partial W}{\partial X} = \frac{\partial T}{\partial X} = 0 \ \text{ at } \ X = \pm\frac{L}{2},\ \ -\frac{B}{2} \le Y \le \frac{B}{2} \ \text{ and } \ 0 \le Z \le H;\\
U(Y = \frac{B}{2}) = U(Y = -\frac{B}{2}),\ \ V(Y = \frac{B}{2}) = V(Y = -\frac{B}{2}),\ \ W(Y = \frac{B}{2}) = W(Y = -\frac{B}{2}),\\
T(Y = \frac{B}{2}) = T(Y = -\frac{B}{2}) \ \text{ at } \ -\frac{L}{2} \le X \le \frac{L}{2} \ \text{ and } \ 0 \le Z \le H,
\end{gathered}$$

when $t > 0$. In the above initial conditions, s is the dimensionless stratification number of the ambient fluid which is defined in the paper.

The above governing equations were discretized on a non-uniform rectangular mesh using a finite volume method, with a standard 2nd-order central difference scheme used for the viscous and divergence terms and the 3rd-order QUICK scheme for the advection terms. The 2nd-order Adams-Bashforth and Crank-Nicolson schemes were used for the time integration of the advective and diffusive terms, respectively. The PRESTO (PREssure STaggering Option) scheme was used for the pressure gradient.

The numerical simulation runs were carried out in the present study using ANSYS Fluent 13. For all numerical simulation runs, the fluid used was water, with the density $\rho_a = 996.6$ kg/m^3, the kinematic viscosity $\nu = 8.58 \times 10^{-7}$ m^2/s, and the volume expansion coefficient $\beta = 2.76 \times 10^{-4}$ 1/K, respectively. X_0 was fixed at 0.002 m, $T_{a,0}$ was fixed at 300 K, the time step was fixed at 0.025 s, but W_0 and T_0 and S_p (which is the dimensional stratification number of the ambient fluid as defined in the paper) were determined from the definitions of Fr, Re and s, with these parameters varying over the ranges of $1 \leq Fr \leq 5$ and $0.1 \leq s \leq 0.5$, all at the fixed $Re = 200$. The dimensions of the computational domain are $H = 0.2$ m, $B = 0.1$ m, and $L = 1.5$ m, which were determined after testing to ensure negligible effects of boundary conditions, particularly the outflows and periodic boundary conditions, on the flow quantities of interest. Non-uniform meshes were used; in the regions of $-25 \leq X/X_0 \leq 25$, $-25 \leq Y/X_0 \leq 25$ and $0 \leq Z/X_0 \leq 50$, a uniform and finer rectangular mesh was used, and in the remaining regions a relatively coarse and non-uniform mesh with varying expansion rates was used.

It should be noted that the "outflow" boundary conditions are applied at the lateral boundaries of the domain (in the X direction, *i.e.*, at the locations $X = \pm L/2$), which assumes a zero diffusion flux for all flow variables. Such a zero diffusion flux condition applied by ANSYS Fluent at "outflow" boundaries is approached physically in fully-developed flows. The "outflow" boundaries can also be defined at physical boundaries where the flow is not fully developed if the assumption of a zero diffusion flux at the exit is expected to have a negligible impact on the flow solution.

Extensive mesh and time-step dependency testing was carried out to ensure accurate simulations to be produced. The results of one example of such testing are presented in Fig. 2 for the case of $Fr = 2$, $Re = 100$ and $s = 0.1$, which shows the horizontal profiles of temperature and vertical velocity at the height of $Z = 0.005$ m in the $X - Z$ plane at the location $Y = 0$, and the vertical profiles of temperature and vertical velocity along the centerline (at $X = Y = 0$) in the Z

direction, all at $t = 20$ s. These results were obtained numerically with three different meshes, with the coarse mesh having 1.17 million cells, the basic mesh having 2.1 million cells and the fine mesh having 3.6 million cells, and at three different time steps of 0.025 s, 0.035 s, and 0.05 s, respectively. It is clear from Fig. 2(a)-(d), where a comparison of the results obtained with the three meshes, all at the same time-step of 0.025 s, is presented, that the results obtained with the basic mesh and the fine mesh are essentially the same and only the results produced with the coarse mesh have some marginal deviations. Similarly, a comparison of the results obtained with four time steps, all with the same basic mesh (2.1 million cells), as shown in Fig. 2(e)-(h), shows that the differences are very small. Hence it is believed that the combination of the basic mesh with 2.1 million cells and the time step at 0.025 s produces sufficiently accurate solutions and is the best compromise between the accuracy and the time and computing resources among the meshes and time steps considered, and is then chosen as the main mesh and time step for the numerical simulations in the present study as the values of Re and Fr are small and the flows are laminar.

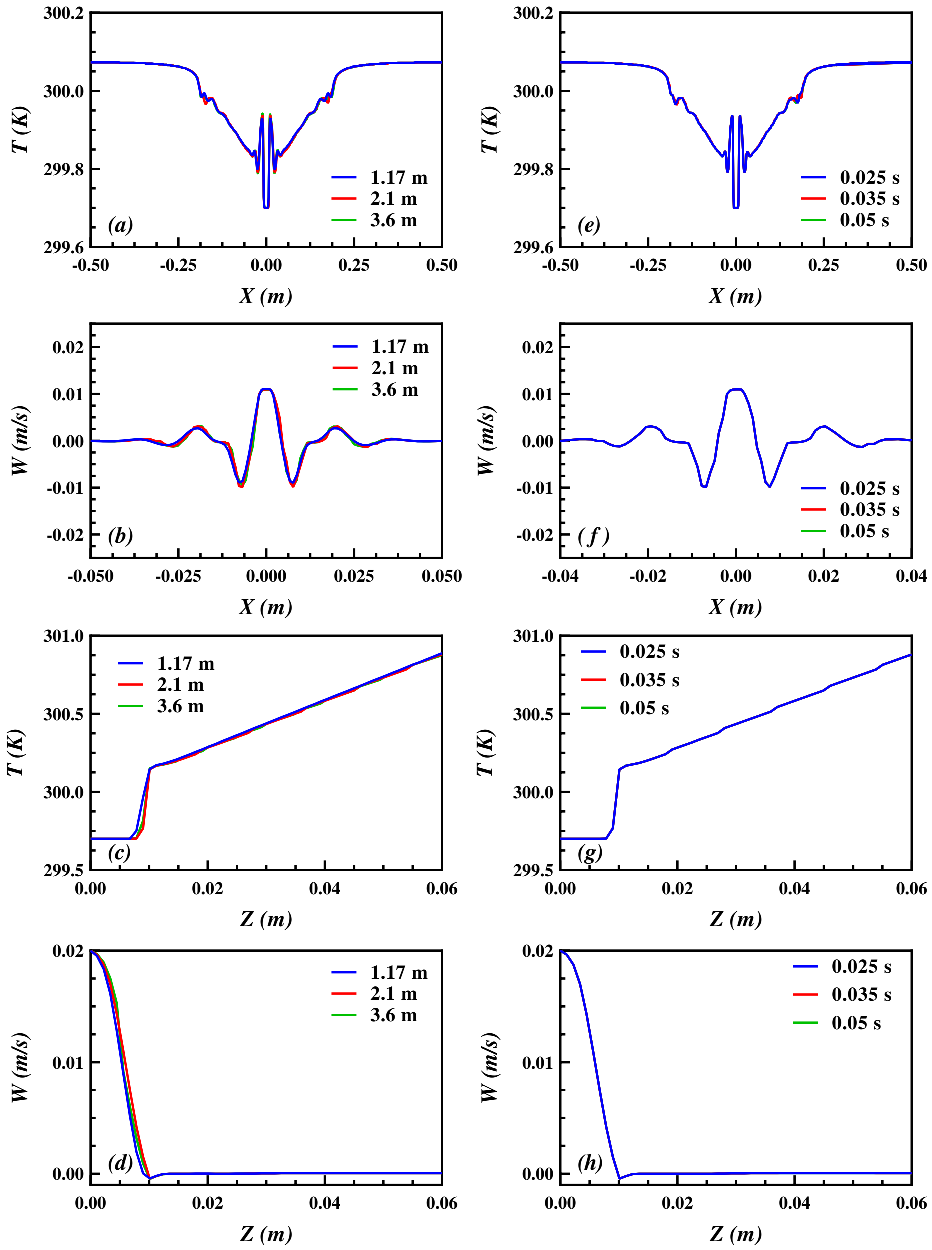

Figure S2: The horizontal profiles of temperature T (K) ((a) and (e)) and vertical velocity W (m/s) ((b) and (f)) at $Z = 0.005$ m in the $X - Z$ plane at the location $Y = 0$, and the vertical profiles of temperature T (K) ((c) and (g)) and vertical velocity W (m/s) ((d) and (h)) along the centerline (at $X = Y = 0$) in the Z direction, all at $t = 20$ s, which were obtained numerically for the case of $Fr = 2$, $Re = 100$ and $s = 0.1$ with three different meshes (left column, all at the same time step of 0.025 s) and at three different time steps (right column, all with the same basic mesh of 2.1 million cells).